Quantum Chemical Study of the Structure, Spectroscopy and Reactivity of NO$^+$.(H$_2$O)$_{n=1-5}$ Clusters

Kirsty A. Linton, Timothy G. Wright and Nicholas A. Besley*

School of Chemistry, University of Nottingham, University Park, Nottingham, NG7 2RD, UK.

E-mail: nick.besley@nottingham.ac.uk

*To whom correspondence should be addressed

Abstract

Quantum chemical methods including Møller-Plesset perturbation (MP2) theory and density functional theory (DFT) have been used to study the structure, spectroscopy and reactivity of $NO^+.(H_2O)_{n=1-5}$ clusters. MP2/6-311++G** calculations are shown to describe the structure and spectroscopy of the clusters well. DFT calculations with exchange-correlation functionals with a low fraction of Hartree-Fock exchange give a binding energy of $NO^+.(H_2O)$ that is too high and incorrectly predict the lowest energy structure of $NO^+.(H_2O)_2$, and this error may be associated with a delocalisation of charge onto the water molecule directly binding to NO^+. Ab initio molecular dynamics (AIMD) simulations were performed to study the $NO^+.(H_2O)_5 \rightarrow H^+.(H_2O)_4 + HONO$ reaction to investigate the formation of HONO from $NO^+.(H_2O)_5$. Whether an intracluster reaction to form HONO is observed depends on the level of electronic structure theory used. Of note is that methods that accurately describe the relative energies of the product and reactant clusters did not show reactions on the time-scales studied. This suggests that in the upper atmosphere the reaction may occur owing to the energy present in the $NO^+.(H_2O)_5$ complex following its formation.

Introduction

The reactivity of the nitrosonium ion (NO^+) and water clusters plays an important role in the chemistry of the ionosphere. The photoionisation of nitric oxide is an essential process in the D layer of the ionosphere and it has been predicted that the major positive ions in the ionosphere are NO^+, O_2^+ and N_2^+, in order of decreasing abundance.[1] Rocket-borne mass spectroscopic experiments have confirmed that NO^+ is present in high abundance in the upper layers of the ionosphere, namely the E layer (90 - 140 km) and F layer (>140 km).[2] However, these measurements unexpectedly found protonated water clusters ($H^+(H_2O)_n$) to be the major positively charged ion present in the lower D layer. Subsequent research has focused on developing an understanding of the high abundance of $H^+(H_2O)_n$ clusters and their formation in the D layer.[3–5] It has been proposed that NO^+ is involved in an associative/dissociative equilibrium with abundant neutral molecules such as X=CO_2,

2

O_2, N_2 or H_2O[3]

$$NO^+ + X + Y \rightleftharpoons NO^+.X + Y \tag{1}$$

where Y is third body. $NO^+.X$ complexes have been detected for all of these species[4] and these complexes can then be involved in a further ligand exchange reaction where X is replaced by a second neutral molecule, such as H_2O.

$$NO^+.X + H_2O \rightleftharpoons NO^+.H_2O + X \tag{2}$$

This two-step hydration process of NO^+ is more efficient than a direct one-step process because of the high concentration of molecules such as N_2 compared with H_2O. Through these reactions, $NO^+.H_2O$ is formed which can then undergo further stepwise solvation to form larger clusters

$$NO^+.(H_2O)_n + H_2O \rightleftharpoons NO^+.(H_2O)_{n+1} \tag{3}$$
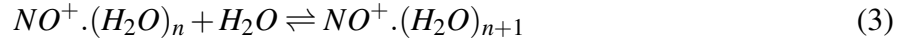
Finally, it was proposed that these clusters could undergo an intracluster rearrangement resulting in the formation of protonated water clusters and nitrous acid.

$$NO^+.(H_2O)_{n+1} \rightarrow H^+.(H_2O)_n + HONO \tag{4}$$

This reaction has been verified experimentally,[6–9] and the detection of small $NO^+.(H_2O)_n$ clusters in the D layer of the ionosphere provides evidence to support this mechanism.[10] In the case of O_2^+, similar intracluster reactions have been proposed that occur at lower values of n[11]

$$O_2^+.(H_2O)_n + H_2O \rightleftharpoons H^+.(H_2O)_n + OH + O_2 \tag{5}$$
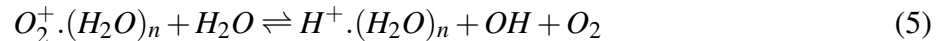
The structure and reactivity of $NO^+.(H_2O)_n$ clusters has been investigated in both experimen-

tal and computational studies. It has been shown that the rate of production of HONO depends on the size and the structure of the water cluster[12] and temperature can also be an important factor since at higher temperatures isomers of higher energy can be present.[13,14] Based on experimental studies, it is believed that nitrous acid, i.e. HONO, formation can occur for $n = 4$ and becomes dominant for $n = 5$.[15,16] DePetris et al. studied the minimum energy structures of $H_2NO_2^+$ and identified six stable minimum energy conformations with Møller-Plesset perturbation theory calculations and concluded that the lowest energy $NO^+.(H_2O)$ structure[17] would be dominant. A full nine-dimensional potential energy surface computed at the coupled cluster theory (CCSD(T)) level has been reported.[18] The surface shows two distinct minima corresponding to the hydrogens of the water molecule being perpendicular to and in the plane of NO^+ with the non-planar structure lower in energy. The structure and vibrational frequencies of $NO^+.(H_2O)_n$ clusters for n in the range 2-5 have been studied by several groups at the MP2, MP4 or coupled cluster levels of theory.[19–22] For the $n = 2$ cluster, MP2 calculations predict that the lowest energy structure has both water molecules bonding to NO^+. A further structure with the second water molecule bonded to the first in the second solvation shell is higher in energy. $NO^+.(H_2O)_n$ clusters have also been studied using density functional theory (DFT). The structure and vibrational spectroscopy of clusters with n=1-3 were studied using molecular dynamics simulations with a generalised gradient approximation (GGA) functional.[23] DFT based Born-Oppenheimer ab initio molecular dynamics (AIMD) have been used to study intracluster reactions leading to the formation of HONO. Most recently, the n=3, 4 and 5 clusters were studied using AIMD simulations with the BLYP+D exchange-correlation functional.[24] No reactions to form HONO were observed for the simulations of the n=3 clusters, while for n=4 clusters reactions were observed and a chain-like isomer was identified as an important intermediate. The larger n=5 clusters were also observed to react with the exception of the most stable isomer. However, some notable differences are observed between the predictions of DFT and correlated wavefunction based methods. This is illustrated by the n=2 cluster where DFT predicts a structure with the second water molecule not directly bonded to NO^+ as the lowest energy structure in contrast to correlated wavefunction methods that predict both water molecules

bound to NO^+. Qualitative differences between DFT and wavefunction based methods are also observed for related systems including ionised water clusters.[25,26] In this paper we investigate the difference between predictions from DFT and MP2 and explore the structure and reactivity of the clusters.

Computational Details

In order to determine the low energy isomers of the $NO^+.(H_2O)_{n=2-5}$ clusters a random search procedure in conjunction with a hierarchical approach was adopted. In the random search procedure, before each structural optimisation cycle the cluster is subjected to twenty random moves in which a molecule in the cluster is chosen at random and rotated by a random angle and translated.[27] For the clusters studied here, up to 150 optimisation cycles were performed. This initial optimisation process was performed at the Hartree-Fock (HF) theory level with the 6-31+G* basis set and generated a large number of structures. The structurally distinct low energy isomers were then re-optimised at the MP2/6-311++G** level of theory and harmonic frequency calculations performed to ascertain if the final structures correspond to minima on the potential energy surface. Finally, the energies of the clusters were determined through single point MP2/aug-cc-pVTZ calculations at the optimised MP2/6-311++G** geometries. Computational infra-red (IR) spectra were generated by convoluting the computed frequencies and intensities with Lorentzian functions. The computed frequencies were scaled by a 0.95 to account for the effects of anharmonicity and other deficiencies in the calculations. Born-Oppenheimer AIMD simulations were performed at a temperature of 220 K with the initial velocities sampled from a Maxwell-Boltzmann distribution and a time step of 0.48 fs. AIMD simulations have been performed at the MP2 level and using DFT with the BLYP-D[28-30] and M06-HF[31] exchange-correlation functionals and a range of basis sets.

Table 1: Computed binding energies with the 6-311++G** basis set and error with respect to CCSD(T) for NO$^+$.H$_2$O in kJ mol^{-1}

Method/Functional	Binding Energy	Error
CCSD(T)	83.98	0.00
HF	83.85	-0.93
MP2	82.67	-1.31
M06-HF	95.25	11.27
PBE50	100.33	16.35
M06-2X	101.86	17.88
ωB97X-D3	105.11	21.13
ωB97X-D	106.65	22.67
PBE0	114.84	30.86
M06	114.97	30.99
B3LYP	115.67	31.69
B3LYP-D	119.36	35.38
M06-L	131.51	47.53
BLYP	134.26	50.28
BLYP+D	138.81	54.83
PBE	140.33	56.35

DFT and MP2 Studies of NO$^+$.H$_2$O and NO$^+$.(H$_2$O)$_2$

Two distinct minima can be identified for the NO$^+$.H$_2$O complex corresponding to planar and non-planar orientations of the water molecule. The energy difference between these two minima is small ($<$0.25 kJ mol^{-1}), but high level calculations confirm that the non-planar structure has the lowest energy.[18] Table 1 shows computed NO$^+$.H$_2$O binding energies for a wide range of exchange-correlation functionals, MP2 and CCSD(T) with the 6-311++G** basis set. The binding energies have been computed with the counterpoise correction, and the error with respect to CCSD(T) is given. The binding energy of 83.98 kJ mol^{-1} for CCSD(T) is consistent with the value of non-counterpoise corrected value of 87.34 kJ mol^{-1} at the CCSD(T)/aug-cc-pV5Z level reported in the literature.[18] The binding energies from DFT vary between 95 and 140 kJ mol^{-1}, all of which are greater than the CCSD(T) value. In contrast, the values from HF and MP2 are in close agreement with CCSD(T). Closer inspection of the DFT binding energies shows a strong correlation between the size of the error and the percentage of HF exchange in the functional. The closest agreement with CCSD(T) is found for the M06-HF, which is a global hybrid functional with

100% HF exchange. Figure 1 shows the lowest energy conformation with the water closest to the nitrogen atom and a non-planar orientation. The figure also shows the net (Mulliken) charge on the two fragments. For the methods with 100% HF exchange, the positive charge is almost entirely localised on NO^+. However, as the fraction of HF exchange is reduced there is an increasing amount of delocalisation of the charge onto the water molecule, with about 30% of the charge on the water molecule for the BLYP functional with or without the dispersion correction. This charge delocalisation is an artefact of the self-interaction error associated with approximate exchange-correlation functionals, and is consistent with these functionals over-estimating the binding energy.

	a^+	b^+
MP2(HF)	0.95	0.05
M06-HF	0.94	0.06
B3LYP	0.78	0.22
BLYP	0.71	0.29
BLYP-D	0.70	0.30
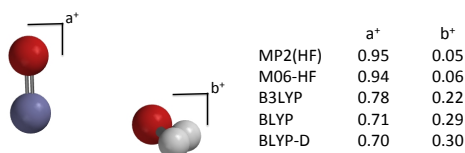
Figure 1: Net charge on NO^+ and H_2O in the $NO^+.H_2O$ complex with different levels of theory with the 6-311++G** basis set.

Figure 2 shows the relative energies of the two dominant low energy structures of $NO^+.(H_2O)_2$ as predicted by MP2, M06-HF and B3LYP with the 6-311++G** basis set. In the first structure (structure 2a) both water molecules are bonded to NO^+, while in the second structure (structure 2b) the second water molecule is bonded to the first and lies in the second solvation shell. For each of these structures there are several structures very close in energy with different orientations of the hydrogen atoms of the water molecules. The MP2 calculations are consistent with previous work[20] where structure 2a has the lowest energy. When zero-point energy (ZPE) is taken into account, the energy difference is about $10\,\text{kJ mol}^{-1}$. The results for the M06-HF are mixed, if ZPE is neglected structure 2a has the lower energy while if ZPE is included structure 2b is favoured. With the B3LYP functional the discrepancy with MP2 is more pronounced and structure 2b is consistently found to be lower in energy by about $7\,\text{kJ mol}^{-1}$. This is initially quite surprising since B3LYP predicts a larger $NO^+.H_2O$ binding energy which would favour binding of both water molecules to NO^+. However, this factor is out-weighed by the the charge delocalisation onto the adjacent

7

water molecule which leads to an artificially high strength of interaction between the two water molecules. This is also evident in the structure 2a′ where there is a clear interaction between the two water molecules that is not observed in the corresponding MP2 structure. In related open-shell species, such as ionised water clusters, the self-interaction error leads to incorrect structures and energetics, and for these clusters the structures are more reliably computed using MP2.[25,26,32] It is interesting to note that similar problems are observed for the closed-shell clusters studied here, and the failure of DFT for the NO^+.Ar complex has been noted previously.[33] Even though the energy difference between the isomers is small, the charge distribution is predicted incorrectly by DFT functionals without a very high fraction of HF exchange, making DFT potentially unreliable for the study of the structures and reactivity of these clusters.

MP2-2a: 0.00   MP2-2b: +5.75

M06-HF-2a: 0.00   M06-HF-2b: +2.87

B3LYP-2a′: 0.00   B3LYP-2b: -6.92
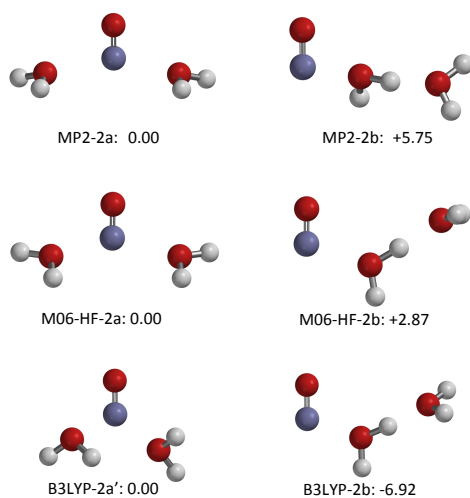
Figure 2: Relative energies (in kJ mol^{-1}) of the two distinct low energy isomers of NO^+.$(H_2O)_2$ including zero point energy, for MP2, M06-HF and B3LYP with the 6-311++G** basis set.

Structure and IR Spectroscopy of NO^+.$(H_2O)_{n=2-5}$

Figure 3 shows the MP2/6-311++G** low energy isomers and associated IR spectra for NO^+.$(H_2O)_2$. Also shown is the lowest energy isomer that contains HONO and H_3O^+. The lowest three energy isomers, 2A, 2B and 2C, are similar with both water molecules bonded to NO^+ but with small differences in the position and orientation of the water molecules. The predicted IR spectra for

8

these isomers for the O-H stretching region agree well with the experimental spectra. We note that the computed spectra have been normalised so that the most intense bands have the same intensity. The computed spectra show two bands, the band at higher frequency corresponds to the asymmetric O-H stretching modes, while the lower frequency band corresponds to the symmetric O-H stretching modes. The spectrum for the cluster with the second water molecule bonded to the first, cluster 2D, has an intense band at 3221 cm^{-1} arising from the O-H bond involved in the hydrogen bond between the two water molecules. There is no evidence of this band in the experimental spectrum indicating that this cluster is not present, and hence that the MP2 calculations correctly predict the lowest energy isomer. The lowest energy isomer with HONO and H_3O^+ has HONO in the trans configuration and lies over 100 kJ mol^{-1} higher in energy when ZPE is included.
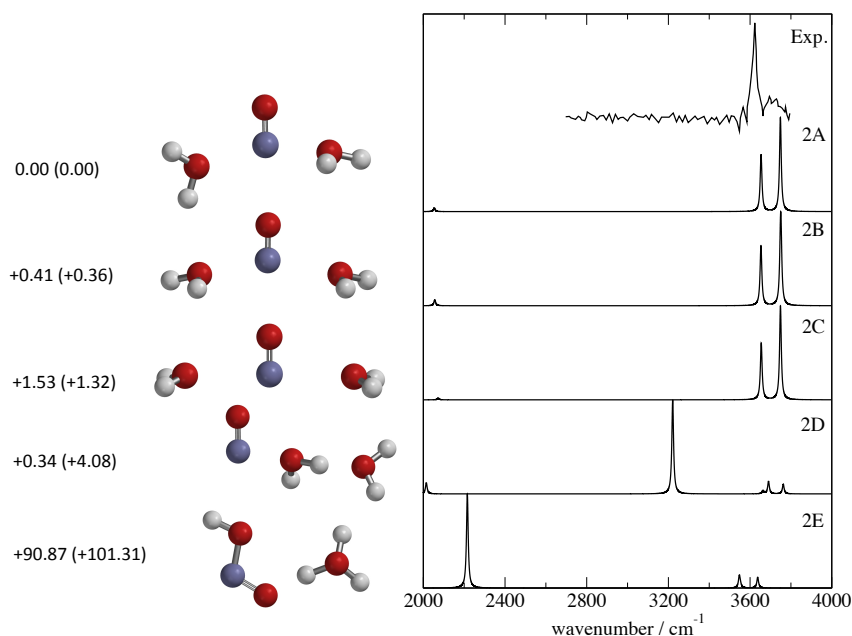
Figure 3: Computed structures and IR spectra for $NO^+.(H_2O)_2$. Experimental IR spectrum adapted from reference,[15] relative energies are given in kJ mol^{-1} with values including zero point energy in parentheses.

The low energy isomers and IR spectra for the $NO^+.(H_2O)_3$ clusters are shown in Figure 4. The lowest energy structure 3A is found to have two water molecules directly bonded to NO^+ with the third water molecule hydrogen bonded between these two water molecules. This structure is

9

consistent with the lowest energy structure found in previous work.[20] The complex with all three water molecules directly bonded to NO^+ is 15.5 kJ mol^{-1} higher in energy, which is reduced to 6.6 kJ mol^{-1} if ZPE is included. Both of these clusters have IR spectra that are similar to the spectrum measured in experiment, and based upon the available IR spectrum it is difficult to distinguish between them. The band at higher frequency has a lower intensity for cluster 3A compared with the spectrum for 3B which is closer to experiment, although the difference in frequency between the two bands is closer to experiment for 3B. At higher energies are clusters where the third water molecule is hydrogen bonded to just one of the water molecules bonded to NO^+. For the higher energy isomers 3C and 3D the distinct bands present in the computed spectra are not observed in experiment suggesting that these clusters are not present. The lowest energy isomer identified that contains HONO, although in this case it is more accurately described as a protonated molecule, HONOH$^+$, lies about 60 kJ mol^{-1} higher in energy than the lowest energy structure. This energy difference is reduced compared with the >90 kJ mol^{-1} for the $n = 2$ clusters and is consistent with the observation that the formation of HONO will become more favourable as n increases.

The $NO^+.(H_2O)_4$ clusters are the smallest cluster where HONO is thought to form. For $n=4$ there are many isomers that lie reasonably close in energy to the lowest energy structure. A large number of these isomers are illustrated in the Supporting Information and here we focus on five distinct structural types. The structures 4A and 4C have very similar energies and the lowest energy structure changes if ZPE is included. Isomer 4A is similar to 3A with the additional water molecule bonding to NO^+, while in 4C all of the water molecules are on the same side of NO^+. The isomer 4A was also identified as the lowest energy isomer in the work of Asada et al.[22] A significant change for $n = 4$ is that the lowest energy isomer with HONO is only 5-8 kJ mol^{-1} higher in energy. In this cluster H_3O^+ is hydrogen bonded to two water molecules and the OH of HONO. At higher energy, cluster 4F has all for water molecules bonded to NO^+. The IR spectra of 4A has a higher frequency band arising from the asymmetric OH stretching modes and a lower frequency band from the symmetric modes. For these large clusters the IR bands have a discernible
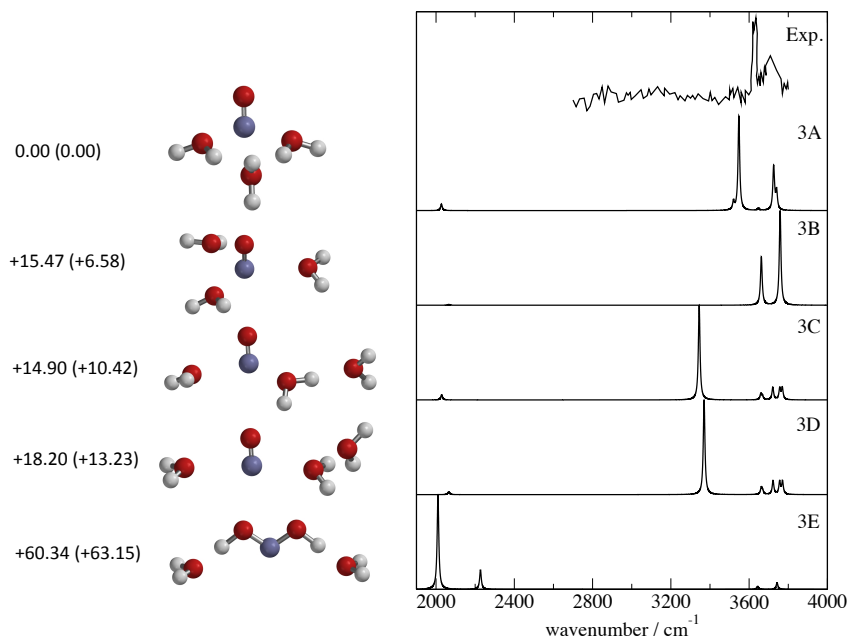
Figure 4: Computed MP2/6-311++G** structures and IR spectra for $NO^+.(H_2O)_3$. Experimental IR spectrum adapted from reference,[15] relative energies are given in kJ mol^{-1} with values including zero point energy in parentheses.

structure arising from water molecules being present in different bonding environments.

Figure 6 shows selected low energy isomers of $NO^+.(H_2O)_5$ with additional structures included in the Supporting Information. The lowest energy structure has the water molecules on one side of NO^+ in agreement with previous work.[22] The computed IR spectrum for this isomer is in good agreement with experiment in the high frequency region. The experimental spectrum also shows an additional intense band at about 2800 cm^{-1}, which is interpreted as evidence for the formation of HONO.[15] The lowest energy isomer with HONO identified in the search has a relative energy of +6.3 kJ mol^{-1} with ZPE included. The computed IR spectrum for this isomer has bands arising from the OH stretching modes of H_3O^+ and is consistent with the interpretation of the experimental spectrum that intracluster reactions have occurred to produce HONO.

11
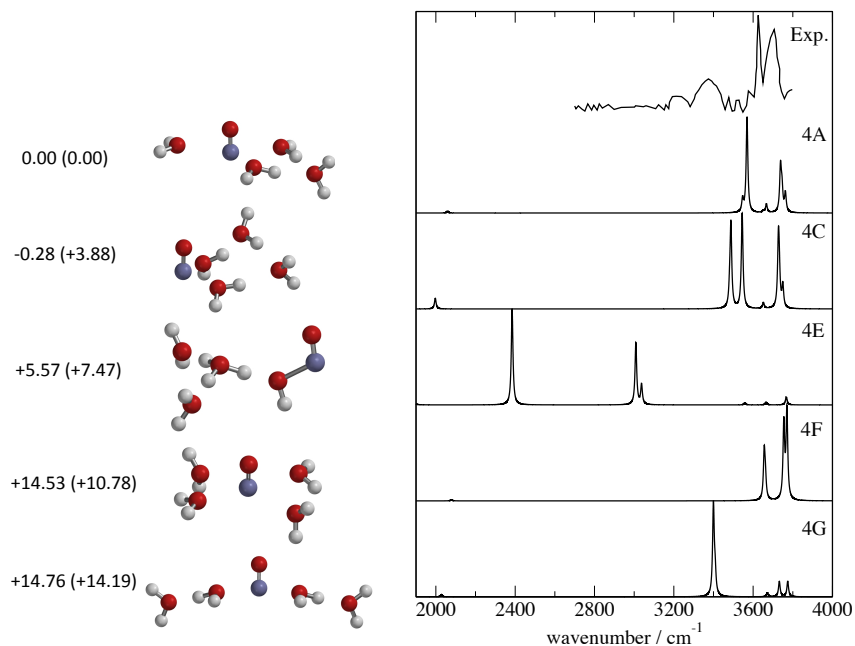
Figure 5: Computed MP2/6-311++G** structures and IR spectra for selected $NO^+.(H_2O)_4$. Experimental IR spectrum adapted from reference,[15] relative energies are given in kJ mol^{-1} with values including zero point energy in parentheses.
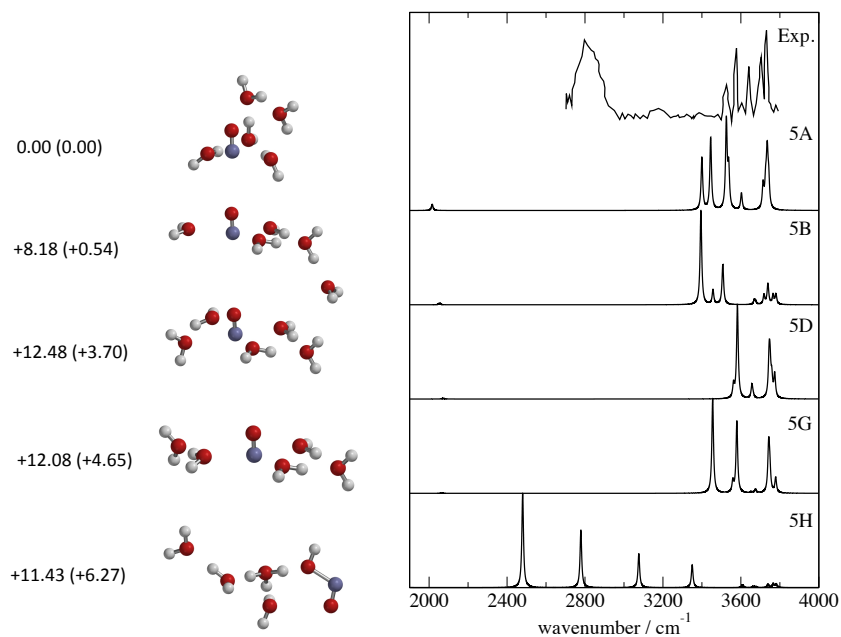
Figure 6: Computed MP2/6-311++G** structures and IR spectra for selected $NO^+.(H_2O)_5$. Experimental IR spectrum adapted from reference,[15] relative energies are given in kJ mol^{-1} with values including zero point energy in parentheses.

Reactivity of $NO^+ \cdot (H_2O)_5$

The results of the previous sections demonstrate that the MP2 with good quality basis sets seems to provide an accurate description of the structure, energetics and IR spectroscopy of the low energy isomers and that the nature of the exchange-correlation functional used in DFT calculations can have a significant effect on the nature of the clusters. There is strong experimental evidence that for clusters with $n = 5$ HONO can be formed, and we now explore the reactivity of the $NO^+ \cdot (H_2O)_5$ with respect to the formation of HONO. AIMD simulations have been performed using structures 5A, 5B, 5D and 5G as initial starting structures at 220 K, which is a typical temperature for the ionosphere, for a range of electronic structure methods. These methods include MP2 and DFT with the M06-HF and BLYP-D exchange-correlation functionals, and these simulations were run with moderately sized (6-31+G*) and small (6-31G) basis sets. Table 3 summarises in which simulations a reaction occurred within the first 2 ps of simulation time. The data show that reactions were only observed for the simulations using DFT with the small basis set. Longer simulations of 4 ps have been performed using BLYP-D/6-31+G* and M06-HF/6-31+G* and still no reactivity was observed. This behaviour can be rationalised by the relative energies of the lowest energy $NO^+ \cdot (H_2O)_5$ cluster and the energy of the cluster with HONO. At the MP2 level with a large basis set, this formation of HONO is unfavourable with a relative energy of +5.8 kJ mol^{-1}. A two point basis set extrapolation of the MP2 aug-cc-pVTZ and aug-cc-pVQZ energies gives a value of +4.7 kJ mol^{-1}. The M06-HF/6-31+G* calculation is consistent with this and predicts the relative energy to be +7.2 kJ mol^{-1}. The BLYP-D/6-31+G* calculations finds the HONO structure to be lower in energy by about 30 kJ mol^{-1}. With the small basis set all methods find the HONO containing cluster to be lower in energy with the DFT calculations predicting a relative energy of about -100 kJ mol^{-1}, and it is this inaccurate description of the energetics of the system that underlies the observed reactivity in the corresponding AIMD simulations.

Notwithstanding the inaccurate relative energies of the small basis set simulations, it is informative to study the details of the reactions. Figures 7 and 8 show the computed energetics with

Table 2: The occurrence of intracluster reactions to form HONO in AIMD simulations of clusters 5A, 5B, 5D and 5G within 2ps at 200 K. R: all reacted, NR: no reactions.

Basis Set \ Method	MP2	M06-HF	BLYP-D
6-31+G*	NR	NR	NR
6-31G	NR	R	R

Table 3: The relative energies of clusters 5A and 5H at different levels of theory.

Method	ΔE / kJ mol^{-1}
MP2/aug-cc-pVQZ	+5.83
MP2/aug-cc-pVTZ	+11.42
MP2/6-31+G*	+22.97
MP2/6-31G	-27.31
M06-HF/6-31+G*	+7.19
M06-HF/6-31G	-105.13
BLYP-D/6-31+G*	-29.96
BLYP-D/6-31G	-97.15

the MP2, M06-HF and BLYP-D methods and 6-311++G** basis set at 200 structures that span the critical time period of the M06-HF/6-31G AIMD simulation in which HONO formations occurs. Also shown is the net charge on the NO fragment evaluated from a natural bonding orbital (NBO) analysis and key structures are highlighted. These are shown for the reactions from the lowest energy $n = 5$ clusters (5A and 5B) with similar energetics for 5A and 5G included in the Supporting Information. For all methods, the energy of the final structure with HONO is higher than the starting structure. This energy change is predicted to be greatest by the MP2 calculations; in addition, the energy barriers are also greater for MP2. Both of these factors suggest that a lower level of predicted reactivity would be expected from MP2 calculations compared with DFT calculations. The two simulations also illustrate different reaction pathways. In the reaction from cluster 5A, there is charge transfer from NO^+ to the water molecules with the formation of H_3O^+ (structures **2** and **3**) before HONO is finally formed. While for 5B there is a more concerted charge transfer from NO^+ and formation of HONO (structure **2**) followed by the making and breaking of the N-O bond until HONO is permanently formed in **3** and **4**. These structures show a chain-like arrangement of the water molecules that was identified as important in earlier work,[24] and these structures are also similar to the stable structures of comparably sized ionised water clusters.[25]

The calculations presented here suggests that no significant reactivity to form HONO from the low energy isomers of $NO^+.(H_2O)_5$ would occur at 220 K. In previous work studying the reactivity of these clusters,[24] reactivity was observed in AIMD with the BLYP-D functional simulations for $n = 4$ clusters and some clusters with $n = 5$. From the simulations presented here, it is clear that the quality of the basis set has a significant influence the occurrence of intracluster reactions to form HONO within the AIMD simulations. Different basis sets were used in the two studies and this is likely to contribute to the different results. One explanation for the observed reactivity to form HONO in experiment may be that when $NO^+.(H_2O)_5$ is formed by the association of an additional water molecule to $NO^+.(H_2O)_4$ the resulting cluster will be locally heated and highly vibrationally excited which would promote reactivity. As shown earlier the binding energy of water to NO^+ is over 80 kJ mol^{-1} which represents a significant amount of energy for the cluster.
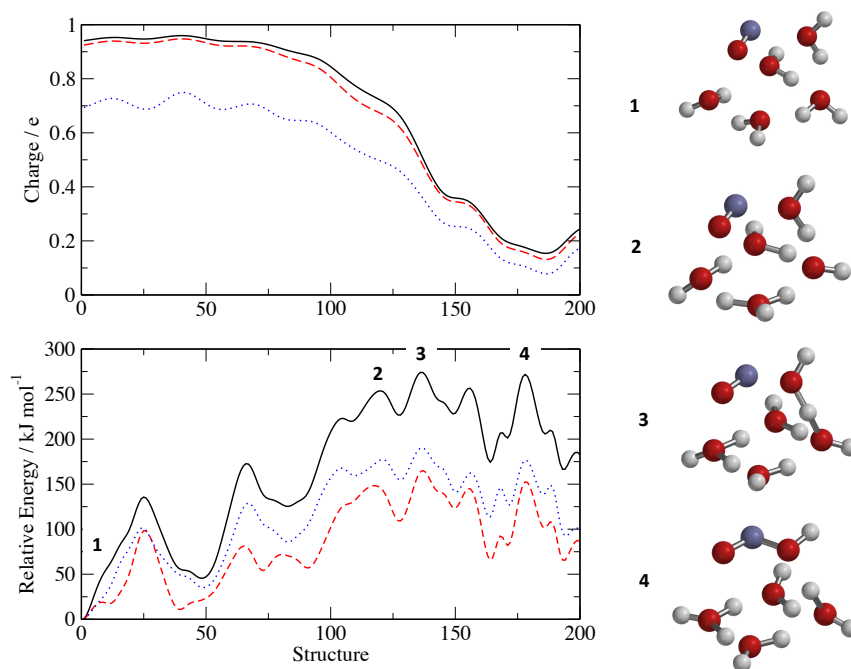
Figure 7: Lower panel: Reaction energy profile for simulation starting at cluster 5A. Upper panel: Net charge on NO. Black line: MP2/6-311++G**, dotted blue line: M06-HF/6-311++G** and dashed red line: BLYP-D/6-311++G**.

15
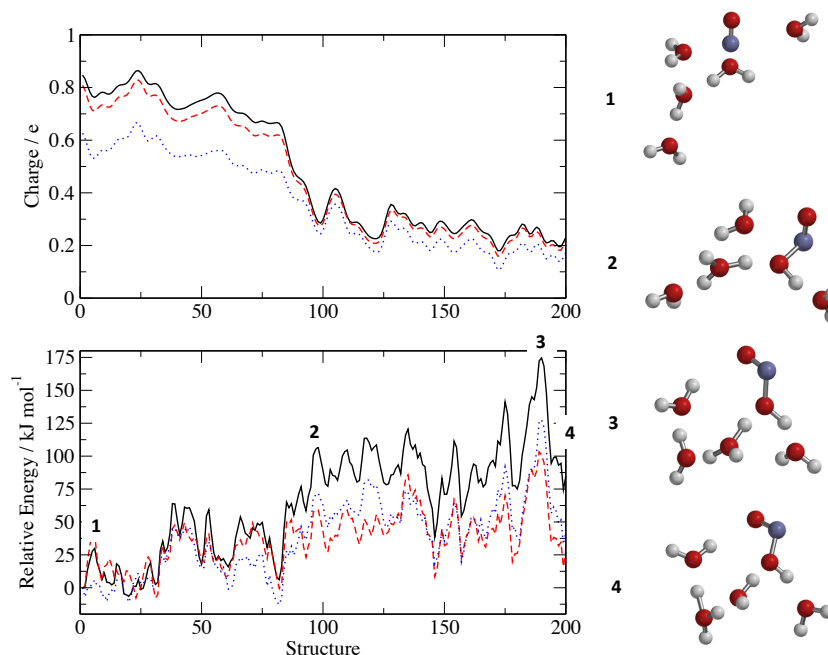
Figure 8: Lower panel: Reaction energy profile for simulation starting at cluster 5B. Upper panel: Net charge on NO. Black line: MP2/6-311++G**, dotted blue line: M06-HF/6-311++G** and dashed red line: BLYP-D/6-311++G**.

Conclusion

As the number of molecules in a molecular cluster increases it becomes challenging to identify the low energy isomers. In this study a random search protocol combined with a hierarchical approach has been employed to determine the low energy structures of $NO^+.(H_2O)_{n=2-5}$ clusters. The structure, energetics and IR spectroscopy of these clusters is shown to be described reliably by MP2 with good quality basis sets such as 6-311++G**. The results of DFT calculations vary significantly with the nature of the exchange-correlation functional. Functionals with a low fraction of HF exchange overestimate the $NO^+.(H_2O)$ binding energy and incorrectly predict the structure of $NO^+.(H_2O)_2$. This can be associated with an artificial delocalisation of charge from NO^+ to water. M06-HF which contains 100% HF exchange provides a more accurate description of the clusters.

Experimental evidence shows that clusters such as $NO^+.(H_2O)_5$ undergo reactions which lead

to the formation of HONO. Predictions of the reactivity of $NO^+.(H_2O)_5$ to form HONO at 220 K based upon AIMD simulations are highly dependent on the electronic structure method used. Long time scale AIMD simulations at the MP2 level are computationally challenging, however, the evidence of this work suggests that reactions leading to the formation of HONO from equilibrated low energy isomers of $NO^+.(H_2O)_5$ are unlikely to occur. One possibility for the observed reactivity in experiment and the ionosphere is that $NO^+.(H_2O)_5$ clusters could be formed from the association of a water molecule to $NO^+.(H_2O)_4$ which would lead to a $NO^+.(H_2O)_5$ cluster with excess energy which would be more conducive to reactivity to form HONO. To explore this further would require extensive AIMD simulations that sample the initial conditions of the cluster.

References

(1) Nicolet A, Aikin AC. (1960) The formation of the D-region of the ionosphere. *J. Geophys. Res.* **65**, 1469-1483.

(2) Narcisi RS, Bailey AD. (1965) Mass spectrometric measurements of positive ions at all altitudes from 64 to 112 kilometers. *J. Geophys. Res.* **70**, 3687-3700.

(3) Dunkin DB, Fehsenfeld FC, Schmeltekopf AL, and Ferguson EE. (1971) 3-body association reactions of NO^+ with O_2, N_2, and CO_2. *J. Chem. Phys.* **54**, 3817-3822.

(4) Arnold F, Krankowsky D. (1979) Mid-lattitude lower ionosphere structure and composition measurements during winter. *J. Atmos. Terr. Phys.* **41**, 1127-1140.

(5) Mack P, Dyke JM, Wright TG. (1997) Calculated thermodynamics of reactions involving NO^+-X complexes (where X=H_2O, N_2 and CO_2). *Chem. Phys.* **218**, 243-256.

(6) Fehsenfeld FC, Ferguson EE. (1969) Origin of water cluster ions in the D region. *J. Geophys. Res.* **74**, 2217-2222.

(7) Lineberger WC, Puckett LJ. (1969) Hydrated positive ions in nitric-oxide-water afterglows. *Phys. Rev.* **187**, 286-291.

(8) Puckett LJ, Teague MW. (1971) Production of $H_3O^+.NH_2O$ from NO^+ precursor in NO-H_2O gas mixtures. *J. Chem. Phys.* **54**, 2564-2572.

(9) Howard C, Rundle H, Kaufman F. (1971) Rates of formation of water clusters for O_2^+ and NO^+. *Bull. Amer. Phys. Soc.* **16**, 213.

(10) Kopp E, Eberhardt P, Herrmann U, Bjorn LG. (1985) Positive-ion composition of the high latitude summer D-region with noctilucent clouds. *J. Geophys. Res.* **90**, 3041-3053.

(11) Angel L, Stace AJ. (1999) Reappraisal of the contribution from $[O_2.(H_2O)_n]^+$ cluster ions to the chemistry of the ionosphere. *J. Phys. Chem. A* **103**, 2999-3005.

(12) Relph RA, Guasco TL, Elliott BM, Kamrath MZ, McCoy AB, Steele RP, Schofield DP, Jordan KD, Viggiano AV, Ferguson EE, Johnson MA. (2010) Network controls proton-coupled water activation in HONO formation. *Science* **327**, 308-312.

(13) Siefermann KR, Abel B. (2010) Ion chemistry mediated by water networks. *Science* **327**, 280-281.

(14) Eyet N, Shuman NS, Viggiano AA, Troe J, Relph RA, Steele RP, Johnson MA. (2011) The Importance of $NO^+(H_2O)_4$ in the conversion of $NO^+(H_2O)_n$ to $H_3O(H_2O)_n$: I. Kinetics measurements and statistical rate modeling. *J. Phys. Chem. A* **115**, 7582-7590.

(15) Choi JH, Kuwata KT, Haas BM, Cao Y, Johnson MS, Okumura M. (1994) Vibrational spectroscopy of $NO^+(H_2O)_n$: Evidence for the intracluster reaction $NO^+(H_2O)_n \rightarrow H_3O^+(H_2O)_{(n-2)}(HONO)$ at $n \geq 4$. *J. Chem. Phys.* **100**, 7153-7165.

(16) Angel L, Stace AJ. (1998) The critical hydration reactions of NO^+ and NO_2^+. *J. Chem. Phys.* **109**, 1713-1715.

(17) De Petris G, Di Marzio A, Grandinetti F. (1991) $H_2NO_2^+$ Ions in the gas phase. A mass spectrometric and post-SCF ab initio study. *J. Phys. Chem.* **95**, 9782-9787.

(18) Homayoon Z. (2014) MULTIMODE quantum calculations of vibrational energies and IR spectrum of the $NO^+(H_2O)$ cluster using accurate potential energy and dipole moment surfaces. *J. Chem. Phys.* **141**, 124311.

(19) Mack P, Dyke JM, Wright TG. (1997) Calculated thermodynamics of reactions involving $NO^+.X$ complexes (where X = H_2O, N_2 and CO_2). *Chem. Phys.* **218**, 243-256.

(20) Hammam E, Lee EPF, Dyke JM. (2000) Ab initio molecular orbital calculations on $NO^+(H_2O)_n$ cluster ions. 1. Thermodynamic values for stepwise hydration and nitrous acid formation. *J. Phys. Chem.* **104**, 4571-4580.

(21) Hammam E, Lee EPF, Dyke JM. (2001) Ab initio molecular orbital calculations on $NO^+(H_2O)_n$ cluster ions. 2. Thermodynamic values for stepwise hydration and nitrous acid formation. *J. Phys. Chem.* **105**, 5528-5534.

(22) Asada A, Nagaoka M, Koseki S. (2011) Ab initio electron correlated studies on the intra-cluster reaction of $NO^+(H_2O)_n$ - $H_3O^+(H_2O)_{n-2}$ (HONO) ($n = 4$ and 5). *Phys. Chem. Chem. Phys.* **13**, 1590-1596.

(23) Ye L, Cheng H.-P. (1998) A quantum molecular dynamics study of the properties of $NO^+(H_2O)_n$ clusters. *J. Chem. Phys.* **108**, 2015-2023.

(24) He R, Lib L, Zhong J, Zhub C, Francisco JS, Zeng XC. (2016) Resolving the HONO formation mechanism in the ionosphere via ab initio molecular dynamic simulations. *Proc. Natl. Acad. Sci. U S A* **113**, 4629-4633.

(25) Do H, Besley NA. (2013) Structure and bonding in ionized water clusters. *J. Phys. Chem. A* **117**, 5385-5391.

(26) Do H, Besley NA. (2013) Proton transfer or hemibonding? The structure and stability of radical cation clusters. *Phys. Chem. Chem. Phys.* **15**, 16214-16219.

(27) Do H, Besley NA. (2012) Structural optimization of molecular clusters with density functional theory combined with basin hopping. *J. Chem. Phys.* **137**, 134106.

(28) Becke AD. (1988) Density-functional exchange-energy approximation with correct asymptotic behavior. *Phys. Rev. A* **38**, 3098-3100.

(29) Lee C, Yang W, Parr RG. (1988) Development of the Colle-Salvetti correlation-energy formula into a functional of the electron density. *Phys. Rev. B Condens Matter* **37**, 785-789.

(30) Grimme S, Antony J, Ehrlich S, Krieg H. (2010) A consistent and accurate ab initio parametrization of density functional dispersion correction (DFT-D) for the 94 elements H-Pu. *J. Chem. Phys.* **132**, 154104.

(31) Zhao Y, Truhlar DG. (2006) Density functional for spectroscopy: No long-range self-interaction error, good performance for Rydberg and charge-transfer states, and better performance on average than B3LYP for ground states. *J. Phys. Chem.* **110**, 13126-13130.

(32) Wadey JD, Besley NA. (2014) The structure and bonding of mixed component radical cation clusters. *Chem. Phys. Lett.* **601**, 110-115.

(33) Wright TG. (1996) Geometric structure of Ar.NO$^+$: Revisited. A failure of density functional theory. *J. Chem. Phys.* **105**, 7579-7582.